

THE INFLUENCE OF STRENGTH AND GRAIN SIZE ON THE MICROSTRUCTURAL CONTROL OF STRESS CORROSION CRACKING OF HIGH STRENGTH STEELS

F. Gutiérrez-Solana*, J. González*, J.M. Varona* and S. Barroso**

This work analyzes the influence that metallurgical variables have on Stress Corrosion Cracking of a High Strength Steel, specially under treatments that promote an intergranular fracture mode. The effect of grain size, strength and, principally, grain boundary structure, as the microstructural determinant of fracture path, are studied. Transition from intergranular to transgranular fracture mode is also analyzed.

INTRODUCTION

The control that microstructure has over the Stress Corrosion Cracking (SSC) of High Strength Steels, has been shown previously (Bernstein and Thompson (1), Thompson and Bernstein (2)). Controlling microstructure can produce important improvements on the SCC resistance of these steels when cracking is transgranular, but it has not been as effective when the fracture process is intergranular (Kerr et al. (3)).

Since more work has to be done to better understand how the metallurgical variables affect the intergranular SCC behaviour of these steels, this work analyzes the influence of grain size and strength of these alloys on their response to intergranular SCC processes, using 3.5% NaCl solution as the aggressive environment. Special attention has been paid to understanding the role played by the morphology of the grain boundary in determining the fracture path.

* E.T.S. Ingenieros de Caminos, Universidad Cantabria, Spain.

** J.E.N. Junta de Energía Nuclear, Madrid, Spain.

FRACTURE CONTROL OF ENGINEERING STRUCTURES – ECF 6

MATERIAL CHARACTERISTICS AND TREATMENTS

The material used in this work is a F.1250 steel (AISI 4135). Its chemical composition can be observed in table 1.

TABLE 1 - Chemical Composition of F-1250 Steel (weight %).

C	S	P	Mn	Si	Cr	Mo
0,34	0,009	0,015	0,72	0,23	0,99	0,16

The steel received was heat treated in different ways in order to get variations in the metallurgical variables which could be analyzed so as to find which microstructural variable(s) determine the intergranular SCC behaviour. Therefore, three different series of heat treatment were performed:

serie A: The coupons of these series were austenitized at five different temperatures varying from 825 to 1000 °C, and then oil-quenched to room temperature, to obtain variation in grain and thus in strength, with a nearly constant microstructure.

serie B: All the coupons in these series were austenitized at 825 °C, then oil-quenched and finally tempered at temperatures varying from 200 °C to 500 °C. This produced material of different strength, due to the variation in microstructure due to tempering.

serie C: The coupons were austenitized at three different temperatures, then oil-quenched and tempered at 400 °C in order to get precipitation at grain boundaries.

TABLE 2 - Heat Treatments performed.

serie A	A1(B0)	825		582
	A2	860		580
	A3	900		567
	A4	950		560
	A5	1000		540
serie B	B0(A1)	825		580
	B1	825	200	540
	B2	825	300	505
	B3	825	400	460
	B4	825	425	440
	B5	825	450	425
	B6	825	500	390
serie C	C0(B3)	825	400	460
	C1	900	400	455
	C2	1000	400	450

FRACTURE CONTROL OF ENGINEERING STRUCTURES – ECF 6

Table 2 summarizes all the treatments done in the three series as well as their Vickers hardness (HV) which is considered to be indirect measurement of strength.

Figure 1 shows the variation of grain size with the temperature of austenitizing. Measurements for the treatments in series A: the specimens are etched with a saturated aqueous solution of picric acid at elevated temperature (80 °C) (Barraclough (4)).

EXPERIMENTAL PROCEDURE AND RESULTS

Mechanical characterization of SCC

To determine the SCC resistance of the steel after the different treatments, half an inch wide DCB samples were machined, pre-cracked by fatigue, and loaded to a constant displacement. Then they were immersed in a 3.5% NaCl solution made with distilled water, which simulate sea-water to initiate SCC.

The test procedure and the way of determining the values of stress intensity factor, K_I , and the crack propagation rate, da/dt , from measurements of crack length, a , has been described previously (Gutiérrez-Solana et al. (5)). The crack length was found from the displacement at the crack mouth, measured by COD gauge. Special attention was paid to determining K_{ISCC} values (stage I), and da/dt in stage II, which is nearly independent of K_I , because these were chosen as the parameters defining the SCC resistance of the material.

As a consequence of the constant deflection, the crack finally arrests, and then the specimen can be used again. In all the samples, at least two complete tests have been run.

Table 3 shows the mean values obtained in each case for the parameters K_{ISCC} and da/dt at $K_I = 30 \text{ MPa } \sqrt{\text{m}}$.

Fractography

Once the test was completed for each specimen, an SEM analysis of fracture surface was done, showing an intergranular character in all cases, except for the specimens tempered at 450 and 500 °C where the fracture mode was transgranular.

TEM ANALYSIS

Considering the important role that grain boundaries should have on the intergranular fracture mode under study, TEM analysis was done using foils obtained from test samples, in order to define the grain boundary morphology. The quenched samples (series A) showed a microstructure composed of dislocated martensite.

FRACTURE CONTROL OF ENGINEERING STRUCTURES – ECF 6

For series A "clean" grain boundaries with no precipitation are observed, showing only differences in thickness from one to other sample.

The tempered samples showed increasing precipitation in both matrix and grain boundaries with temperature, due to the tempering.

TABLE 3 - Results of Mechanical Characterization of SCC.

specimen	K_{ISCC} (MPa \sqrt{m})	da/dt (ms^{-1}) $K_I=30$ MPa \sqrt{m}	plastic zone size (r_y) at		grain size / plastic zone size (d/r_y)
			K_{ISCC}	$K_I=30$	at K_{ISCC}
A1	9.9	1.5×10^{-6}	1.35	12.3	22
A2	11.7	1.3×10^{-6}	1.9	12.5	23
A3	13.6	1.7×10^{-6}	2.67	13.1	28
A4	15.1	1.3×10^{-6}	3.38	13.4	29
A5	16.8	1.6×10^{-6}	4.5	14.2	32
B0(A1)	9.9	1.5×10^{-6}	1.35	12.3	22
B1	12.5	1.5×10^{-6}	2.5	14.3	12
B2	16.1	1.5×10^{-6}	4.7	16.4	6.5
B3	19.8	1.3×10^{-6}	8.6	19.7	3.5
B4	22.5	0.3×10^{-8}	12.1	21.6	2.5
B5	75	4.2×10^{-8} *	144.7	-	0.207
B6	130	4×10^{-8} **	516.5	-	0.058
C0	19.8	1.3×10^{-6}	8.6	19.7	3.5
C1	20	1.4×10^{-6}	9	20.2	8.4
C2	18.2	1.1×10^{-6}	7.6	20.7	20

* for $K_I = 100$ MPa \sqrt{m}

** for $K_I = 150$ MPa \sqrt{m}

ANALYSIS OF THE RESULTS

The results obtained have been correlated with the metallurgical variables analyzed, showing the following relations. Figure 2 shows the variation of the defined SCC resistance parameters, K_{ISCC} and da/dt at stage II, with the austenitizing temperature.

FRACTURE CONTROL OF ENGINEERING STRUCTURES – ECF 6

The increasing values of K_{ISCC} are related to grain size (figure 3) and strength (figure 4). The results follow the general rule that SCC resistance increases as strength decreases. In this case, a 7% decrease in strength caused by increasing grain size, a increased K_{ISCC} by 60%.

Figure 2 shows that no changes in propagation rate are produced by varying the austenitizing temperature of quenched specimens.

Figure 5 shows the variation of SCC parameters for samples of series as a function of tempering temperature. The results are compared with the results obtained for the quenched samples austenitizing at the same temperature (825 °C). As can be seen, the K_{ISCC} values increase with tempering temperature in a smooth way up to 425 °C from 10 to 20 MPa \sqrt{m} , and then suddenly to 70 MPa \sqrt{m} at 450 °C and over 100 MPa \sqrt{m} , at 500 °C. This step is associated with the change in surface fracture appearance from intergranular to transgranular.

Again, no changes in propagation rate were observed with increasing tempering temperature, as long as the mode of fracture was intergranular: values were the same as those in quenched samples. Once the fracture mode is transgranular the propagation becomes much slower, by up to 30 times. The gradual improvement in SCC behaviour with the tempering temperature can be correlated with the associated loss of strength due to microstructural changes in tempering, as can be observed in figure 6. As the microstructural variation and the corresponding strength do not present discontinuities, the steps observed in both SCC parameters, K_{ISCC} and da/dt , must be caused by the change from intergranular to transgranular modes.

For serie C samples, figure 7 shows the K_{ISCC} and da/dt variation with the austenitizing temperature, which principally changes the grain size. As can be seen, no variation of K_{ISCC} and da/dt values were obtained, indicating a constant SCC behaviour for these samples.

DISCUSSION

The analysis of the results obtained in the mechanical characterization of SCC of the three series of samples treated showed different correlations that should be discussed.

K_{ISCC} variation

The K_{ISCC} variation observed in quenched samples of series A cannot be explained by geometrical effects. Gonzales et al. (6) have proposed that grain boundaries form an obstacle to expanding the

hydrogen affected zone. Assuming that the latter is the same as the plastic zone, they proposed a fixed ratio between grain size and plastic zone size at K_{ISCC} . Figure 8 shows the actual variation of grain size to plastic zone size ratio for the quenched samples tested.

The only structural change observed with conventional TEM analysis on grain boundaries of these quenched samples was their thickness, which variation correlates with that of K_{ISCC} as can be seen in figure 9. The size of the plastic zone increases with austenizing temperature (table 3) both because of the increase in K_{ISCC} and the reduction in strength. These two effects suggest that the rupture of quenched samples depends on a critical deformation of the grain boundary: the critical value being changed by hydrogen produced in SCC (Gonzales et al. (7))

For the tempered samples it has been mentioned that the step observed in K_{ISCC} values at the range 425-500 °C of tempering temperatures cannot be justified by the corresponding microstructural changes. To better understand this situation, which is associated with the intergranular-transgranular change in fracture mode, table 3 shows the variation of K_{ISCC} with the ratio grain size/plastic zone size. In all the intergranular cases this ratio decreases continuously as the temperature of tempering increases (K_{ISCC} increases) upto the value of 2.5 where there is a change in the micromechanisms controlling rupture. For transgranular cracking this ratio drops much lower than one, indicating that the plastic zone covers a number of grains during crack propagation. This change in the ratio grain size/plastic zone size has previously been associated with the corresponding changes in fracture mode (Kerr et al. (3)). See figure 10.

Microstructural changes due to tempering over this range of temperatures affect the SCC behaviour because it is transgranular. The changes in intergranular behaviour can be justified by the presence of precipitates at grain boundaries, which varies with temperature.

These precipitates can suffer decohesion at a critical concentration of hydrogen trapped by them (Pressouyre (8)), so changes in precipitation as well as plastic zone size (due to strength variation) can affect the corresponding value of K_{ISCC} . In the case of the samples in series C, tempering is carried out at the same temperature, so that the same kind of precipitate is present in each. This is why there is no change in K_{ISCC} values.

Propagation rate, da/dt

All differences observed in propagation rate in all the samples treated are associated with the intergranular to transgranular change in mode of fracture. In all the intergranular cases the propagation rate is about 1 to $2 \cdot 10^{-6}$ m/s. Considering that the propagation phenomena can be controlled by hydrogen diffusion to crack tip, and that the fracture paths are the grain boundaries, grain-boundary hydrogen diffusion may be important.

By contrast, when the fracture mode is transgranular slower propagation rates are obtained, varying greatly with treatment down to values around $4 \cdot 10^{-8}$ m/s. This slower and variable propagation rate may be because hydrogen must diffuse through the lattice, which is slower and depends on the presence of traps in the microstructure. (Pressouyre (9), Gutiérrez-Solana et al. (10)).

CONCLUSIONS

The study of intergranular SCC process on this steel showed the important effects of the metallurgical variables such as grain size and strength, on K_{ISCC} values. However, these factors only work indirectly on the local criterion for fracture of the grain boundary, which is the ultimate controlling factor. Different correlations have been obtained for quenched and tempered samples according with the absence or presence of precipitation on grain boundaries. At the same time no variation in propagation rates have been observed.

Finally, the important changes in SCC behaviour are caused by the transition from intergranular to transgranular fracture. This, they are not associated with sudden changes in the metallurgical parameters but with the change in the controlling mechanisms.

ACKNOWLEDGEMENTS

This work is included in a Research Program funded by the Comision Asesora para la Investigación Científica y Técnica (CAICYT) of the Ministerio de Educación y Ciencia of Spain.

SYMBOLS USED

HV	= Vickers hardness
K_I	= stress intensity factor (MPa \sqrt{m})
a	= crack length
δ	= load line displacement (m)
$K_{I\text{SCC}}$	= threshold value of K_I at stage I (MPa \sqrt{m})
da/dt	= crack propagation rate (ms^{-1})
d	= grain size (μm)
r_y	= plastic zone size (μm)
δ_{gb}	= thickness of grain boundary (μm)

REFERENCES

- (1) Bernstein, I.M. and Thompson, A.W., Int. Metals Reviews, Vol. 21, 1976, pp. 269-287.
- (2) Thompson, A.W. and Bernstein, I.M., Advances in Corrosion Science and Technology, Vol. 7, 1980, pp. 53-173.
- (3) Kerr, R., Gutiérrez-Solana, F., Bernstein, I.M. and Thompson, A.W., "The Role of Microstructure on the SCC of Medium to High Strength Steels." Submitted for publication in Metallurgical Transactions.
- (4) Barraclough, D.R., Metallography, Vol. 6, 1973, pp. 465-472.
- (5) Gutiérrez-Solana, F., Bernstein, I.M. and Thompson, A.W., Proceedings of 6th Asamblea del CENIM, Madrid, Spain. Edited by CENIM, 1985, artículo 164.
- (6) González, J., Gutiérrez-Solana, F. and Varona, J.M., Anales de Ingeniería Mecánica, Vol. 3, 1985, pp. 239-243.
- (7) González, J., Private communication from his work for Ph.D.
- (8) Pressouyre, G.M. "Current solutions to Hydrogen Problems in Steels". Proceeding of "Current Solutions to Hydrogen Problems in Steel" Washington, U.S.A., Edited by Interrante, C.G. and Pressouyre, G.M., A.S.M., 1982, pp. 18-37.
- (9) Pressouyre, G.M., Thesis, Ph.D., Carnegie-Mellon University, Pittsburg, 1977.
- (10) Gutiérrez-Solana, F., Bernstein, I.M. and Thompson, A.W. Proceedings of 6th Asamblea del CENIM, Madrid, Spain. Edited by Cenim, 1985, Artículo 163.

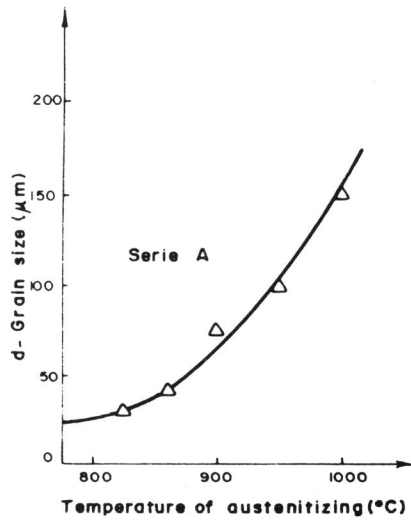


Figure 1.- Grain size variation with austenitizing temperature.

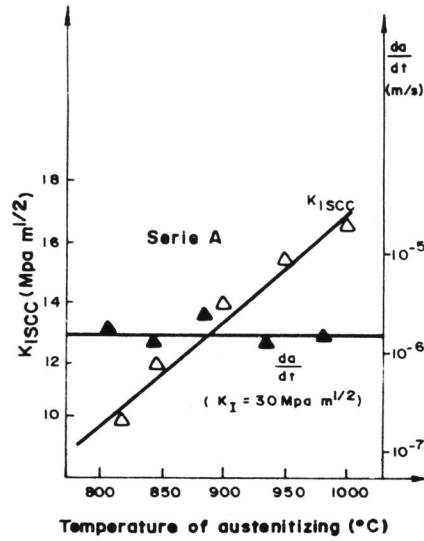


Figure 2.- SCC parameters variation with austenitizing temperature in serie A.

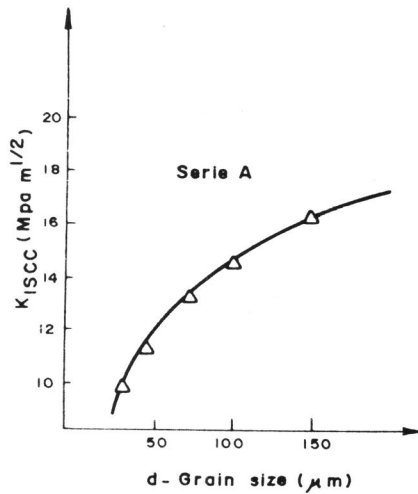


Figure 3.- $K_{I\text{SCC}}$ variation with grain size of serie A specimens.

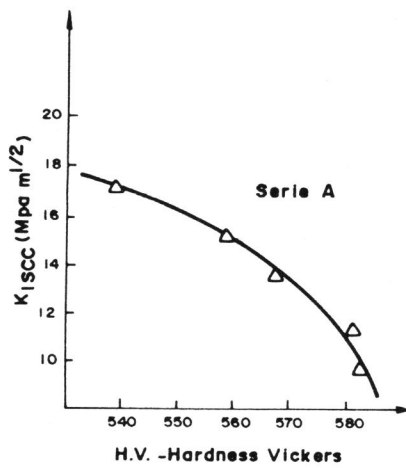


Figure 4.- $K_{I\text{SCC}}$ variation with strength of serie A specimens.

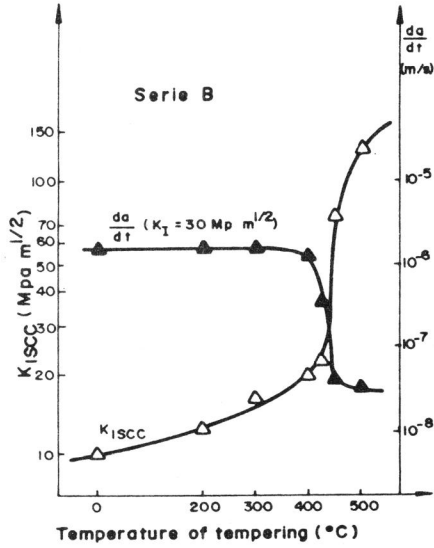


Figure 5.- SCC parameters variation with tempering temperature in serie B.

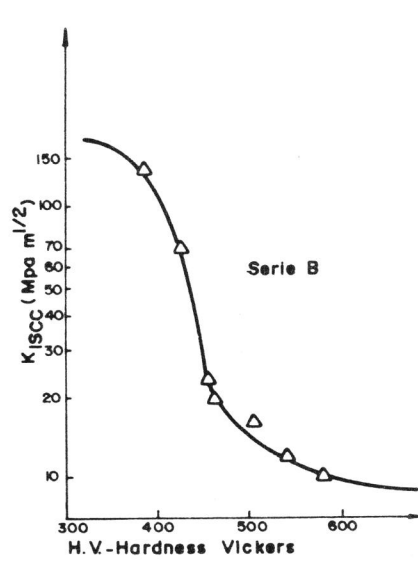


Figure 6.- $K_{I\text{SCC}}$ variation with strength of serie B specimens.

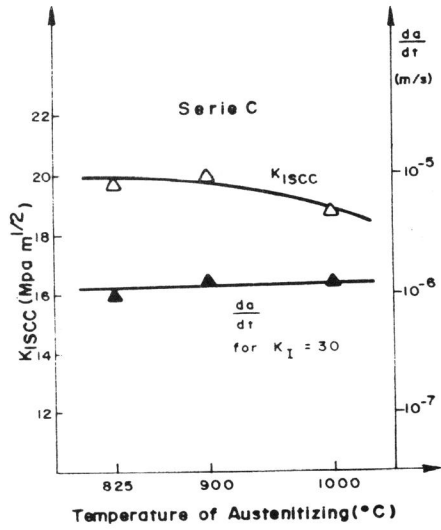


Figure 7.- SCC parameters variation with austenitizing temperature in serie C.

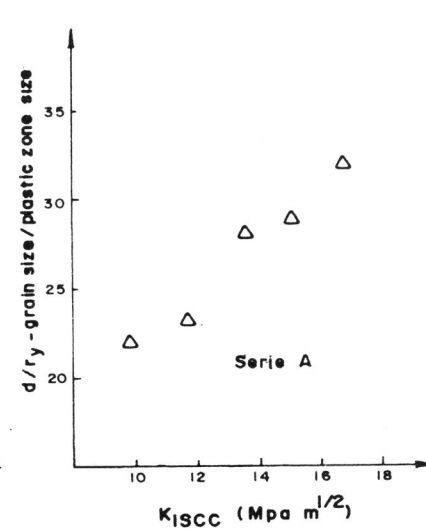


Figure 8.- Grain size/plastic zone size ratio variation with $K_{I\text{SCC}}$ values of quenched samples.

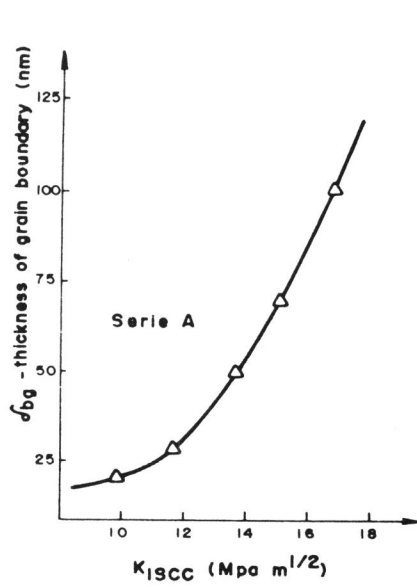


Figure 9.- K_{ISCC} variation with thickness of grain boundary of quenched samples.

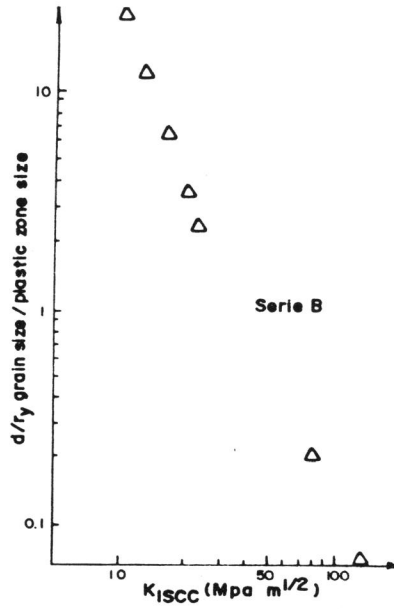


Figure 10.- Grain size/plastic zone size ratio variation with K_{ISCC} values of tempered samples.